A Simplified Interference Model for Outdoor Millimeter Wave Networks

Xiaolin Jiang[1(✉)], Hossein Shokri-Ghadikolaei[1], Carlo Fischione[1], and Zhibo Pang[2]

[1] KTH Royal Institute of Technology, Stockholm, Sweden
{xiaolinj,hshokri,carlofi}@kth.se
[2] ABB Corporate Research, Västerås, Sweden
pang.zhibo@se.abb.com

Abstract. Industry 4.0 is the emerging trend of the industrial automation. Millimeter-wave (mmWave) communication is a prominent technology for wireless networks to support the Industry 4.0 implementation. The availability of tractable accurate interference models would greatly facilitate the design of these networks. In this paper, we investigate the accuracy of an interference model that assumes impenetrable obstacles and neglects the sidelobes. We quantify the error of such a model in terms of statistical distribution of the signal to noise plus interference ratio for outdoor mmWave networks under different antenna array settings. The results show that assuming impenetrable obstacle comes at almost no accuracy penalty, and the accuracy of neglecting antenna sidelobes can be guaranteed with sufficiently large number of antenna elements.

Keywords: Millimeter-wave network · Interference model
Simplicity-accuracy tradeoff · Interference model accuracy index

1 Introduction

Industry 4.0, or the fourth industrial revolution is the current trend of the industrial automation [1]. It is based on the base of Internet of Things, which enables the industrial modules to communicate and cooperate with each other in real time. The industrial manufacturing requires high reliability and stringent delay guarantee, and is usually realized by the wired communication. However, to support mobility, flexibility, and to get rid of the heavy and expensive cables, wireless communication is the promising solution for the future deployment [2].

Millimeter wave (mmWave) is a potential technology for wireless communication network of Industry 4.0, as it has abundant bandwidth to support high data rate, which is essential for the applications to transmit the real-time video [3]. Moreover, as the delay spread of mmWave is lower than the microwave band, which is helpful to reduce the guard interval for the inter symbol interference mitigation. This can efficiently improve the transmission efficiency, especially for the machine to machine type communication transmitting short packets [4].

M. Huang et al. (Eds.): WICON 2016, LNICST 214, pp. 101–108, 2018.
https://doi.org/10.1007/978-3-319-72998-5_11

The availability of accurate interference models is essential to evaluate the performance of mmWave networks. However, exact or very accurate interference models are generally quite complex and sometimes mathematically intractable. Interference models with different accuracy and complexity have been used in the literature. A simple interference model considering infinite penetration loss and no sidelobe transmission/reception is used to develop multihop medium access control layer in mmWave wireless networks [5]. This simple interference model enables deriving tractable closed-form expressions for the main performance metrics and delivering useful design insights. However, the accuracy of the underlying interference model is not therein quantified. In [6], the blockage is modeled by a line-of-sight (LOS) ball, i.e., all the transmitters within a certain distance of the receiver are always in the LOS condition, and all the other transmitters have a non-LOS condition. This approximation greatly simplifies mathematical analysis. This blockage model is extended to a more complex two-ball model with better accuracy in [7]. The accuracy of such interference model comes at the price of complexity and less tractability. In [8], an index is proposed that allows quantifying the accuracy of any interference model.

In this paper, we assess the accuracy of the simple interference model of [5], namely assuming impenetrable obstacles and no antenna sidelobes. We investigate the accuracy index defined in [8] and the relative difference in 50th percentile rate under a uniform planar array (UPA) of antennas at 28 GHz. The results show that the assumption of impenetrable obstacles introduces negligible loss in the accuracy of the interference model, thanks to the special characteristics of the mmWave communications. Moreover, considering no sidelobes may cause non-negligible accuracy loss with small antenna size, which can be compensated by increasing the number of antenna elements.

2 System Model

We consider a downlink scenario for an outdoor network operating at the mmWave frequencies. The number of BSs and obstacles are random variables with densities λ_b and λ_o per square kilometer respectively, and they are randomly uniformly distributed in the plane, as shown in Fig. 1. We assume that

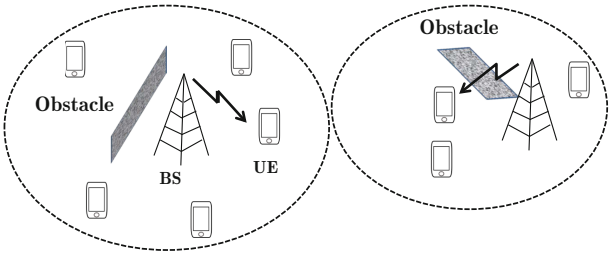

Fig. 1. Outdoor mmWave network. The dashed lines show the base station coverage boundaries, and may not be that regular in practice.

each obstacle has a rectangular shape with a random width that is independently uniformly taken from [0,5] m, a random length uniformly taken from [0,10] m, and a random orientation that is independently uniformly taken from $[0, 2\pi]$. We study the performance of a reference user UE 0 located at the origin of the Cartesian coordinate, which will be associated to the BS with the smallest pathloss. We consider a single path narrowband geometrical channel model between every BS to its serving UE [4]. Then, the downlink channel response between BS i and UE j is given by

$$\mathbf{H}_{ij} = \sqrt{N_t N_r} g_{ij} \mathbf{a}_{\mathrm{UE}} \left(\phi_{ij}^{\mathrm{UE}}, \theta_{ij}^{\mathrm{UE}}\right) \left(\mathbf{a}_{\mathrm{BS}} \left(\phi_{ij}^{\mathrm{BS}}, \theta_{ij}^{\mathrm{BS}}\right)\right)^{*}, \tag{1}$$

where N_t and N_r are the number of antenna elements at the transmitter side and at the receiver side, ϕ_{ij}^{UE} and $\theta_{ij}^{\mathrm{UE}}$ are the horizontal and vertical angles of arrival (AoA) at the UE j from BS i, ϕ_{ij}^{BS} and $\theta_{ij}^{\mathrm{BS}}$ are the horizontal and vertical angles of departure (AoD) from the BS i to UE j, $\mathbf{a}_{\mathrm{BS}} \left(\phi_{ij}^{\mathrm{BS}}, \theta_{ij}^{\mathrm{BS}}\right)$ and $\mathbf{a}_{\mathrm{UE}} \left(\phi_{ij}^{\mathrm{UE}}, \theta_{ij}^{\mathrm{UE}}\right)$ are normalized array responses to the AoD and AoA along this link, and $(\cdot)^*$ is the Hermitian operator. Without loss of generality, we consider half-wavelength UPAs of size $N_b \times N_b$ at the BSs and of size $N_u \times N_u$ at the UEs. For half wavelength UPA of $N \times N$ antennas, we have [9]

$$\mathbf{a}\left(\phi, \theta\right) = \frac{1}{N}[1, \ldots, e^{j\pi(m \sin\phi \, \sin\theta + n \cos\theta)}, \ldots, e^{j\pi((N-1)\sin\phi \, \sin\theta + (N-1)\cos\theta)}]^{*}, \tag{2}$$

where $0 \leq m < N$, and $0 \leq n < N$ are the indices of an antenna element along the two dimensions in the UPA array. The term g_{ij} in (1) is a zero-mean complex Gaussian random variable with variance $10^{-0.1 L_{ij}}$, where L_{ij} is the path loss in dB [4]. Let d_{ij} be the distance between BS i and UE j (path length) in meters, n_{ij} be the number of obstacles in this path, l_o be the penetration loss of each obstacle in dB, α be the attenuation factor due to atmospheric absorption, and $l_\alpha = 10 \log(e^{\alpha d_{ij}})$ be the absorption loss in dB, which is 1.15×10^{-5} at 28 GHz. Then, the path loss is

$$L_{ij}\,[\mathrm{dB}] = c + 20 \log(d_{ij}) + l_\alpha + n_{ij} l_o + X\,, \tag{3}$$

where c is a constant attenuation, and equals 61.4 dB at 28 GHz, X is a zero-mean i.i.d. Gaussian random variable with standard deviation $n = 5.8$ dB.

We assume a universal frequency reuse, so all non-serving BSs can cause interference to UE 0. The associated BS is indexed by 0, and the set of all interfering BSs is denoted by $\mathcal{I}$. Then, the SINR at UE 0 is

$$\gamma = \frac{p_0 \left| \left(\mathbf{w}_0^{\mathrm{UE}}\right)^{\mathrm{H}} \mathbf{H}_{00} \, \mathbf{w}_0^{\mathrm{BS}} \right|^2}{\sum\limits_{i \in \mathcal{I}} p_i \left| \left(\mathbf{w}_0^{\mathrm{UE}}\right)^{\mathrm{H}} \mathbf{H}_{i0} \, \mathbf{w}_i^{\mathrm{BS}} \right|^2 + \sigma}\,, \tag{4}$$

where p_i is the transmission power of BS i, σ is the noise power, $\mathbf{w}_0^{\mathrm{UE}}$ is the combining vector at UE 0, and $\mathbf{w}_i^{\mathrm{BS}}$ denotes the precoding vector at BS i.

To reduce the complexity and cost of beamforming, we assume an analog precoder both at the BSs and at the UEs; however, the framework of this paper can be easily extended to other beamforming strategies. At each BS, the transmitting beam is matched to the AoD direction to its associated UE. Similarly, the combining vector at each UE i is matched to the AOA from its serving BS. That is given BS i will serve UE j, $\mathbf{w}_i^{\mathrm{BS}} = \mathbf{a}_{\mathrm{BS}}\left(\phi_{ij}^{\mathrm{BS}}, \theta_{ij}^{\mathrm{BS}}\right)$ and $\mathbf{w}_j^{\mathrm{UE}} = \mathbf{a}_{\mathrm{UE}}\left(\phi_{ij}^{\mathrm{UE}}, \theta_{ij}^{\mathrm{UE}}\right)$. This precoding and combining vectors can maximize the link SNR, namely $|(\mathbf{w}_j^{\mathrm{UE}})^* \mathbf{H}_{ij} \mathbf{w}_i^{\mathrm{BS}}|^2$, see [10].

An interference model attempts at modeling different components of (3). For mathematical tractability, usually, antenna pattern or channel models are simplified. These approximations make it possible to evaluate the SINR distribution and thereby performance metrics such as the data rate. However, the derived SINR distribution may not necessarily be close to the actual SINR distribution before all those approximations. In the next section, we introduce two metrics that allow quantifying the closeness of two statistical distributions.

3 Measuring Accuracy of SINR and Rate Analysis

Consider a reference interference model y, which results in SINR γ^{y} with distribution $f_{\gamma^{\mathrm{y}}}(t)$, and any test interference model x, which results in SINR γ^{x} with distribution $f_{\gamma^{\mathrm{x}}}(t)$. In the following, we consider the interference model accuracy index [8] and the relative difference in the 50th percentile rate.

3.1 Interference Model Accuracy Index

The interference model accuracy (IMA) index describes how close the PDF of γ^{x} is compared to PDF of γ^{y}. To formally define IMA index, let $\beta > 0$ denote the SINR threshold corresponding to a certain target bit error rate, then an outage on the receiver occurs when $\gamma < \beta$. Suppose that the interference model y can perfectly capture outage events. Let hypotheses H_0 and H_1 denote the absence (i.e., $\gamma^{\mathrm{y}} \geq \beta$) and the presence (i.e., $\gamma^{\mathrm{y}} < \beta$) of outage under reference model y. For any constant $0 \leq \xi \leq 1$, the interference model accuracy index is defined as

$$\mathrm{IMA}\left(\mathrm{x}, \mathrm{y}, \xi, \beta\right) = \xi\left(1 - p_{\mathrm{fa}}^{\mathrm{x}|\mathrm{y}}(\beta)\right) + (1-\xi)\left(1 - p_{\mathrm{md}}^{\mathrm{x}|\mathrm{y}}(\beta)\right), \tag{5}$$

where $p_{\mathrm{fa}}^{\mathrm{x}|\mathrm{y}}(\beta) = \Pr\left[\gamma^{\mathrm{x}} < \beta \mid \gamma^{\mathrm{y}} \geq \beta\right]$ is the false alarm probability, and $p_{\mathrm{md}}^{\mathrm{x}|\mathrm{y}}(\beta) = \Pr\left[\gamma^{\mathrm{x}} \geq \beta \mid \gamma^{\mathrm{y}} < \beta\right]$ is the miss-detection probability. $\mathrm{IMA}\left(\mathrm{x}, \mathrm{y}, \xi, \beta\right)$ is a unitless real-valued quantity ranging within $[0, 1]$, where higher values represent higher similarity between x and y. By setting $\xi = \Pr\left[\gamma^{\mathrm{y}} \geq \beta\right]$, parameter $\mathrm{IMA}\left(\mathrm{x}, \mathrm{y}, \Pr\left[\gamma^{\mathrm{y}} \geq \beta\right], \beta\right)$ is equal to the average probability that interference model x gives the same decision as the reference model y.

We define the minimum IMA index as,

$$\min \mathrm{IMA}\left(\mathrm{x}, \mathrm{y}\right) = \min_{\beta}\ \mathrm{IMA}\left(\mathrm{x}, \mathrm{y}, \Pr\left[\gamma^{\mathrm{y}} \geq \beta\right], \beta\right)\ . \tag{6}$$

The term $\min \mathrm{IMA}\left(\mathrm{x}, \mathrm{y}\right)$ shows the minimum value (worst case) of the accuracy of interference model x compared to the reference model y.

3.2 The Relative Difference in the 50th Percentile Rate

The transmit data rate is an important index to assess the network performance. We consider maximum achievable rate as

$$\text{Rate} = \text{B}\log_2(1+\gamma), \tag{7}$$

where B is the bandwidth and γ is the SINR. The rate coverage as the complementary cumulative distribution function of rate is

$$P(\rho) = \Pr(\text{Rate} > \rho), \tag{8}$$

where ρ is the rate threshold that determines different rate coverage values. Denote the 50th percentile rate calculated by interference model x and y by $\rho^{\text{x}}_{50\text{th}}$ and $\rho^{\text{y}}_{50\text{th}}$, respectively. Besides rate coverage, we calculate the relative difference in the 50th percentile rates calculated by two interference models x and y as a metric of accuracy of rate analysis:

$$\text{Rate}_{\text{diff}-50\%} = \frac{|\rho^{\text{x}}_{50\text{th}} - \rho^{\text{y}}_{50\text{th}}|}{\rho^{\text{y}}_{50\text{th}}}. \tag{9}$$

The parameter $\min \text{IMA}$ ranges within $[0, 1]$ with higher value representing better similarity, while $\text{Rate}_{\text{diff}-50\%}$ ranges within $[0, \infty]$ with smaller value representing better similarity.

4 Simplified Interference Model for Outdoor MmWave Networks

Interference models in mmWave networks are generally very complicated due to both blockage and directionality. Simplifying the blockage model and antenna patterns, as done in [5], will significantly increase tractability of mathematical performance evaluation and optimization of mmWave networks, and can lead to better design insights. These insights are valid as long as the underlying simple interference model is of sufficient accuracy. In the following, we investigate the accuracy of such interference model.

We consider a "realistic" reference physical model y with a finite penetration loss and actual antenna pattern, created by the analog precoding and combining vectors. We then approximate such simplified interference model by x wherein we consider infinite penetration loss and no antenna sidelobes.

To evaluate the effect of infinite penetration loss assumption, we consider a test model x_a with $l_o = \infty$ in (3). Other parameters of x_a are similar to those of y. To evaluate the effect of the no-sidelobe approximation, we take a test model x_b similar to y except that the sidelobe gain is ignored in x_b. The 28 GHz band is 27.5–29.5 GHz, and in the following and without loss of generality, we consider 30 dBm transmission power, 500 MHz bandwidth (so −87 dBm noise power).

4.1 Impact of Assuming Infinite Penetration Loss

In this subsection, we evaluate the impact of assuming impenetrable obstacles on the SINR distribution. Figure 2 shows min IMA against the penetration loss in y (it is always ∞ in x_a). To calculate min IMA, we sweep β from 0 to 30 dB to capture the smallest accuracy value in this SINR threshold region. From this figure, assuming impenetrable obstacles is more accurate for higher penetration loss values. Moreover, the accuracy index increases with the density of BSs, as more BSs is equivalent to shorter distances between the interfering BSs and UE 0, and higher likelihood of having interferes with LOS condition to the UE 0. For penetration loss less than 15 dB, the assumption of impenetrable obstacle reduces min IMA by less than 1% when the obstacle density is $20/\text{km}^2$. On the other hand, the accuracy index expectedly decreases with the density of obstacles. The accuracy loss, however, is very limited, e.g., only 1% additional loss when increasing the obstacle density from $20/\text{km}^2$ to $50/\text{km}^2$ for the penetration loss of 5 dB. Even this such small loss vanishes when the penetration loss is larger than 35 dB.

Figure 3 shows $\text{Rate}_{\text{diff}-50\%}$ between y and x_a. Similarly as Fig. 2, $\text{Rate}_{\text{diff}-50\%}$ decreases with the density of BSs, and minimal difference exists when $\lambda_b = 50/\text{km}^2$ and penetration loss larger than 15 dB. Overall, the assumption of impenetrable obstacles introduces negligible loss in calculating SINR and

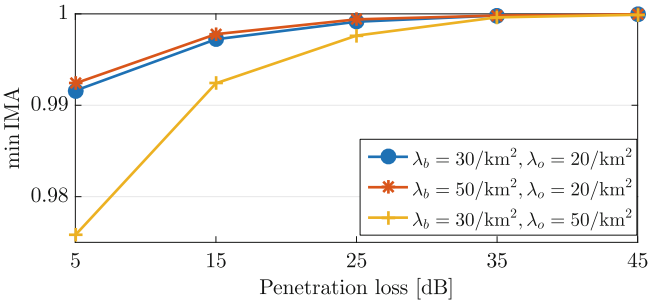

Fig. 2. Impact of infinite penetration loss on min IMA.

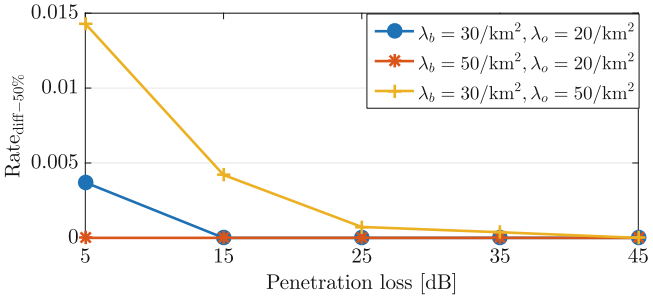

Fig. 3. Impact of infinite penetration loss on $\text{Rate}_{\text{diff}-50\%}$.

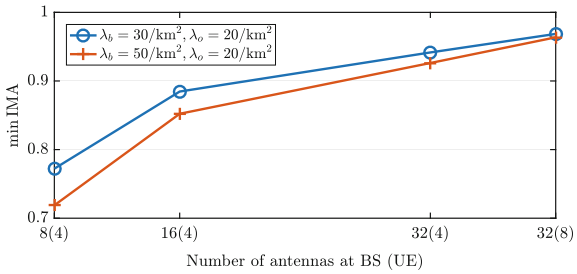

Fig. 4. Impact of ignoring antenna sidelobes on min IMA. Antenna elements are in the form of UPA of N×N antennas.

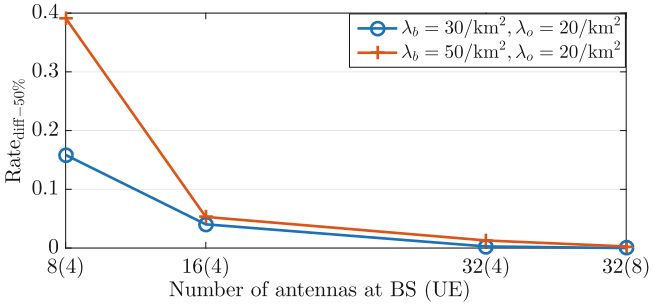

Fig. 5. Impact of ignoring antenna sidelobes on $\text{Rate}_{\text{diff}-50\%}$. Antenna elements are in the form of UPA of N×N antennas.

rate distributions, but improves the mathematical tractability. This assumption works very well in mmWave networks with denser BS deployments.

4.2 Impact of Neglecting Antenna Sidelobes

Figure 4 presents the effect of neglecting the sidelobes. The antenna patterns at BSs and UEs are set as the parameters at the x label. Neglecting the sidelobes can lead to clear difference between x_b and y. The accuracy index increases with the number of antennas at each side, as more antennas enable narrower beamwidth and less sidelobe gain, e.g., the min IMA indexes increase from 0.73 to 0.96, and from 0.86 to 0.97 respectively with the antenna number increase from 8×8 UPA to 32×32 UPA at BSs, and 4×4 UPA to 8×8 UPA at UEs in the two scenarios. It is also observed that the min IMA index decreases with more interfering BSs, as the increased aggregated interferes lead to less similarity between the two models.

Ignoring antenna sidelobes can also introduce a noticeable difference to the rate distribution, as shown in Fig. 5. With dense BS deployment and moderate number of antennas at both BS and UE, $\text{Rate}_{\text{diff}-50\%}$ is as large as 39%. With the increase of the number of the antenna elements, $\text{Rate}_{\text{diff}-50\%}$ of the two scenarios decrease to around 5% when using 16×16 UPA at the BS side.

5 Conclusions

We proposed a simplified interference model in outdoor mmWave networks that considers infinite penetration loss and no sidelobe. Then we investigated the similarity of SINR and rate distributions between this simplified model with realistic model using an interference model accuracy index and the relative difference in the 50th percentile rate. The impact of the first assumption on the accuracy of the simplified interference model can be neglected, while the impact of considering no sidelobe can not be neglected in denser BS settings. However, by increasing the number of antennas can increase the accuracy. The accuracy index can be further improved by effective frequency reuse and proper scheduling to limit the number of interfering BSs transmitting simultaneously. The simplified interference model can be a good base for the research of other techniques in mmWave networks such as beamforming and association between BSs and UEs.

References

1. Schwab, K.: The fourth industrial revolution. World Economic Forum, Geneva (2016)
2. Willig, A., Matheus, K., Wolisz, A.: Wireless technology in industrial networks. Proc. IEEE **93**(6), 1130–1151 (2005)
3. Rangan, S., Rappaport, T.S., Erkip, E.: Millimeter-wave cellular wireless networks: potentials and challenges. J. Proc. IEEE **102**(3), 366–385 (2014)
4. Akdeniz, M.R., Liu, Y., Samimi, M.K., Sun, S., Rangan, S., Rappaport, T.S., Erkip, E.: Millimeter wave channel modeling and cellular capacity evaluation. J. IEEE J. Sel. Areas Commun. **32**(6), 1164–1179 (2014)
5. Singh, S., Ziliotto, F., Madhow, U., Belding, E., Rodwell, M.: Blockage and directivity in 60 GHz wireless personal area networks: from cross-layer model to multihop MAC design. J. IEEE J. Sel. Areas Commun. **27**(8), 1400–1413 (2009)
6. Singh, S., Kulkarni, M.N., Ghosh, A., Andrews, J.G.: Tractable model for rate in self-backhauled millimeter wave cellular networks. J. IEEE J. Sel. Areas Commun. **33**(10), 2196–2211 (2015)
7. Di Renzo, M.: Stochastic geometry modeling and analysis of multi-tier millimeter wave cellular networks. J. IEEE Trans. Wireless Commun. **14**(9), 5038–5057 (2015)
8. Shokri-Ghadikolaei, H., Fischione, C., Modiano, E.: On the accuracy of interference models in wireless communications. In: IEEE International Conference on Communications, Kuala Lumpur, pp. 1–6 (2016)
9. El Ayach, O., Rajagopal, S., Abu-Surra, S., Pi, Z., Heath, R.W.: Spatially sparse precoding in millimeter wave MIMO systems. J. IEEE Trans. Wireless Commun. **13**(3), 1499–1513 (2014)
10. El Ayach, O., Heath, R.W., Abu-Surra, S., Rajagopal, S., Pi, Z.: The capacity optimality of beam steering in large millimeter wave MIMO systems. In: 13th IEEE International Workshop on Signal Processing Advances in Wireless Communications, Cesme, pp. 100–104 (2012)